11th International Conference on Fracture Mechanics of Concrete and Concrete Structures
FraMCoS-11
J. M. Chandra Kishen, A. Ramaswamy, S. Ray and R. Vidyasagar (Eds)

UNCERTAINTY IN THE SIMULATION OF CONCRETE FRACTURE AND COMPARISON WITH BLIND COMPETITIONS

JAN CERVENKA[*], VLADIMIR CERVENKA[*], ULVIS SKANDIS[†] AND LUBOS REHOUNEK[††]

[*] Cervenka Consulting s.r.o.(CC)
Na Hrebenkach 55, 150 00, Praha, Czech Republic
e-mail: jan.cervenka@cervenka.cz, www.cervenka.cz

[†] Latvia University of Life Sciences and Technologies, Dep. of Struct. Eng. (LBTU)
Jelgava, Latvia
e-mail: ulvis@lbtu.lv, www.lbtu.lv

[††] Czech Technical University, Dept. of Mechanics (CETU)
Thakurova 6, Prague, Czech Republic
lubos.rehounek@fsv.cvut.cz

Key words: Simulation, Reinforced Concrete, Uncertainty, Concrete Fracture

Abstract: Fracture mechanics based nonlinear analysis of reinforced concrete structures is becoming a standard engineering tool for the assessment of existing structures as well as for the design of new structures. This development is supported by the introduction of new safety formats for nonlinear analysis in the fib model code 2010, which are being implemented in the new version of Eurocodes prEN 1992 1 1:2022.

An important aspect is the evaluation and treatment of all uncertainties involved. The paper focuses on the treatment of model uncertainty. Interesting insight into the uncertainty of fracture mechanics based modelling can be obtained by studying several recent blind prediction competitions.

The blind predictions are useful for the assessment of the robustness and reliability of existing models or software tools. Their specifics and limits will be demonstrated using five recent prediction competitions. The main deficiency is that material uncertainty is usually not addressed; therefore, the most accurate predictions are usually pure lucky shots.

1 INTRODUCTION

The application of finite element method for nonlinear analysis of reinforced concrete structures has been introduced already in the 70`s by landmark works of Ngo & Scordelis [1], Rashid [2] and Červenka V. & Gerstle [3]. Many types of material models of reinforced concrete were developed in 70's, 80's and 90's such as for instance Suidan & Schnobrich [4], Lin & Scordelis [5], De Borst [6], Rots & Blaauwendrad [7], Pramono & Willam [8], Etse [9], Lee & Fenves [10] or Červenka [11]. These models are typically implemented in finite element software and a concrete material model is applied at each integration point for the evaluation of internal forces. The crack band method introduced by Bažant and Oh [12] is often used to decrease the mesh size dependency and eliminate the spurious zero energy dissipation when element size approaches zero.

The application of nonlinear finite element method for the design and assessment of reinforced concrete structures offers engineers an important insight into the realistic behavior of their structures. Advanced material models can evaluate the crushing of concrete when subjected to high compressive stress as well as cracking, when the tensile strength is exceeded.

Furthermore, for the reinforcement material, yielding and rupturing can be simulated. By these means, a complex assessment of the structural performance is feasible.

The development of new safety formats for nonlinear analysis and their introduction to the engineering codes for design and assessment of reinforced concrete structures [13] greatly enhances the application of fracture mechanics based nonlinear analysis into the engineering practice. This increases the importance of proper treatment of model uncertainty.

2 MODEL UNCERTAINTY

The evaluation of model uncertainty of the resistance based on nonlinear finite element analysis (NLFEA) is important for the robust and reliable application in design. The model uncertainty can be determined by comparing model predictions to experimental data. The obtained partial factors of model uncertainty are valid only for the investigated material model or simulation software. The model uncertainty is usually defined as the ratio:

$$\theta = R_{\text{exp}} / R_{\text{sim}} \tag{1}$$

where R_{exp} is the resistance found by an experiment and R_{sim} is the resistance obtained by a numerical simulation. The model uncertainty is considered as an additional random variable with a lognormal distribution.

The experimental resistance is considered as a reference, i.e. true value. Other effects such as aleatory uncertainties should be reduced to minimum. Material properties of concrete are typically identified by the concrete compressive strength tested on small samples (e.g. cylinders). Other material parameters (elastic modulus, tensile strength, fracture energy, etc.) are usually determined indirectly by formulas available in codes or should be provided as guidelines for a particular model. The model uncertainty should be evaluated by comparing the numerical results with a suitable experimental database.

The evaluation of the model uncertainty using a database of 33 reinforced concrete members with different failure modes is described in more detail by Červenka et al. [14]. This study was using the software ATENA [15] with the fracture-plastic concrete material model [11][16]. The obtained model uncertainty parameters are summarized in Table 1. Other studies of model uncertainty for other models and finite element software codes were for instance performed by Engen [17], Castaldo [18][19] and Gino [20]. The obtained uncertainty factors were mostly in the range 1.02 – 1.19 except for the study [19], which included also cyclic load cases, and the model uncertainty factor 1.35 was obtained.

Table 1: Partial safety factors for model uncertainty (Červenka V. [14])

Failure type	μ_θ	V_θ	γ_{Rd}
Punching	0.971	0.076	1.16
Shear	0.984	0.067	1.13
Bending	1.072	0.052	1.01
All failure modes	0.979	0.081	1.16

These uncertainty factors should be included in any applications of NLFEA in engineering practice and should be used to reduce the structural or member resistances calculated by numerical simulation.

3 BLIND COMPETITIONS

Software developers apply significant financial and human resources to the testing and validation of their products, and the evaluation of model uncertainty should be included in this effort.

The software testing and validation as well as the model uncertainty evaluation is typically performed using an existing database of already known experimental results. This involves a significant risk that the analyst will adjust certain material or solution parameters to obtain a better match and lower model uncertainty safety factor. In the case of reinforced concrete, the analyst typically knows only the concrete compressive strength, the bar diameters and the reinforcement yield and tensile strength. This is usually not enough for an accurate analysis of reinforced concrete and other parameters are necessary. These parameters need to be derived from the compressive strength or other data by clear rules and formulas that shall be fixed during the model uncertainty quantification.

It is therefore very useful and interesting to participate in blind robin competitions on predicting the response of reinforced concrete structures that are often organized by various research institutions.

Such competitions have certain limitations as well. They often involve a single experiment; therefore, they include the influence of both aleatory (inherent uncertainty due to randomness of input data) and epistemic (missing knowledge) uncertainty mixed together.

The authors participated in the past in various blind competitions, and in this paper the results of 5 recent competitions are summarized and discussed. These competitions involved altogether 8 different tests mostly involving shear behavior or RC members. One case also contains a pre-stressed element, and one case deals with very interesting steel fiber reinforced concrete material. All presented results have been calculated using software ATENA [15] and the fracture-plastic concrete material model described in more detail in [11][16].

3.1 Deep shear test Toronto/UC Berkeley

The first group of blind predictions involves two very similar experiments. One was organized by Toronto University by Prof. Collins and Bentz in 2015.

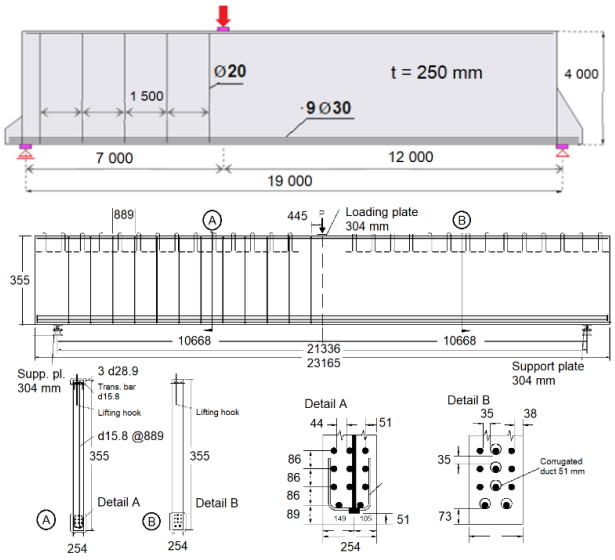

Figure 1: Test geometries (units in mm) for the Toronto (2015, [21]) and UC Berkeley beams (2021, [22]).

Detailed description of the test and the prediction results are in the publication [21]. A similar beam was also tested in the contest organized by UC Berkeley [22] Very large beams were tested with the span over 19 m and the height of 3.5 - 4 m as is shown in Figure 1.

Table 2: Material parameters for the blind competitions of Toronto and UC Berkeley.

Parameter	Toronto	UC Berkeley
Concrete		
Elastic modulus **E** [MPa]	34129	31 008
Poisson ratio	0.2	0.2
Compressive strength $\mathbf{f_c}$ [MPa]	40.0	30
Tensile strength $\mathbf{f_{ct}}$ [MPa]	3.0	2.3/2.4(*)
Fracture energy $\mathbf{G_F}$ [N/m]	78	100/135(*)
Crushing lim. displ. $\mathbf{w_d}$ [mm]	5	20
Fixed cracks	1.0	0.75/1.0(*)
Strength reduction of cracked concrete r_c^{lim}	0.8	1.0/0.8(*)
Shear factor s_F	50	50/20(*)
Reinforcement		
Elastic modulus **E** [MPa]	200 000	200 000
Yield strength $\mathbf{f_{ys}}$ [MPa]	573/522(**)	830/420(**)
Tensile strength $\mathbf{f_{ts}}$ [MPa]	685/629(**)	1030/620(**)
Limit strain ε_{s2} [-]	0.18/0.2(**)	0.025/0.02(**)

(*) The second value indicates the default value normally generated by the software for the given strength class. The results using these parameters are indicated by the label "default".

(**)The first value is for the shear reinforcement, the second for the longitudinal bars.

Very similar geometry and approach was adopted in both cases. In the UC Berkeley test, during the first test, i.e. in the right side, four longitudinal bottom reinforcement bars were left unbonded inside the beam (see Detail B, Figure 1). This was not the case with the Toronto test. After the first test was completed, these bars were injected with grout for the second test, i.e. loading of the left side. This

means that each beam consisted of two tests: first loading up to failure in the right side. Then the right side was strengthened with steel ties, and the second test was performed of the left side with shear reinforcement.

The material parameters used in the analysis are listed in Table 2.

The author's predictions for the two competitions are shown in Figure 2 and Figure 3, and for the Toronto competition, they were the winning predictions. They are indicated by the solid lines in Figure 2.

The predictions for the UC Berkeley competition (Figure 3) were not so satisfactory. Especially for the test without shear reinforcement, i.e. the curve labeled "Sim. Right" in Figure 3 has a peak almost 50% lower than in the experiment labeled as "Exp. Right".

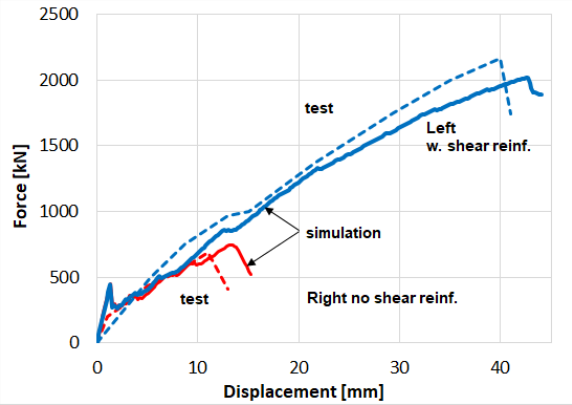

Figure 2: Toronto test prediction and experiment comparison.

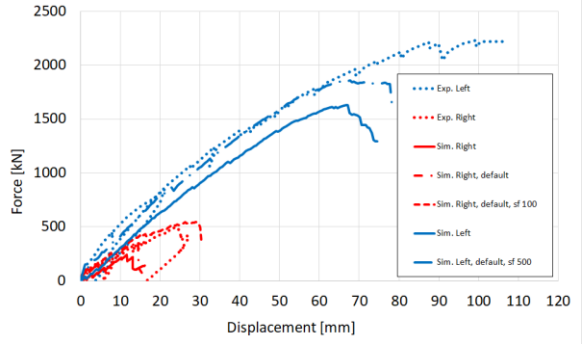

Figure 3: UC Berkeley test prediction and experiment comparison.

It should be however considered that the self-weight of the beam is significant especially for the test without shear reinforcement, i.e. "Exp. Right". This is valid also for the Toronto test.

In UC Berkeley experiment, for instance, the self-weight of the beam is about 515 kN. This means that the peak load was in reality underestimated by only about 25% for "Exp. Right" and 22% for the "Exp. Left". It is also necessary to understand that there was only a single experiment performed in both cases so uncertainty in the material parameters, i.e. aleatory uncertainty was not addressed in the test at all. In both cases, the failure was dominated by concrete diagonal cracking.

Especially in the "Exp. Right" the tensile properties played the major role, while in the "Exp. Left" it was the concrete compressive crushing as well as the steel yielding controlling the peak load. This means that quite high variability of the structural strength can be expected namely in the "Right" test just from the material heterogeneity and variability.

However, the major source of inaccuracy in the UC Berkeley prediction was the consideration of shrinkage (150 μ-strains), which by itself reduced the beam strength of the "Sim. Right" by about 25%.

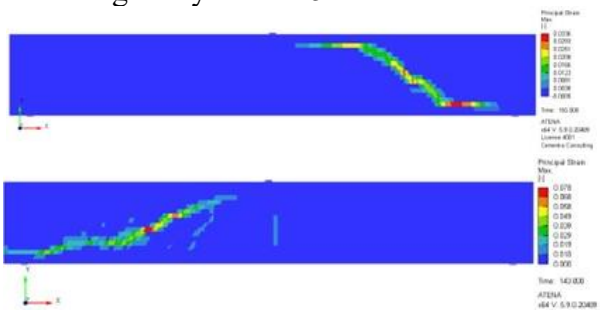

Figure 4: Crack pattern for the UC Berkeley beam predictions.

This is documented by the curve denoted as "Sim. Right - default", where default material parameters of the software were used, and shrinkage was not considered. The error of this analysis was only 12% considering the dead weight. Important parameter for the shear dominated problems is the shear factor parameter s_F [16], which controls the shear stiffness of the cracked concrete, which had to be increased to 100 in order to have a good match with the experiment. This analysis is denoted as "Sim. Right, default, s_F 100" in Figure 3. The default value of this parameter is normally set to 20 to provide conservative results. The typical crack patterns for the two UC Berkeley experiments are shown in Figure

4, and they are in very good agreement with the observed failure modes.

3.2 Cyclic column UC Berkeley

Gunay and Donald [23] organized a competition in 2021 at UC Berkeley on the response of reinforced concrete column in cyclic behavior.

The geometry of the tested column is shown in Figure 5, and material properties used in the simulation are listed in Table 3. Details of the experiment and competition results can be found in [23].

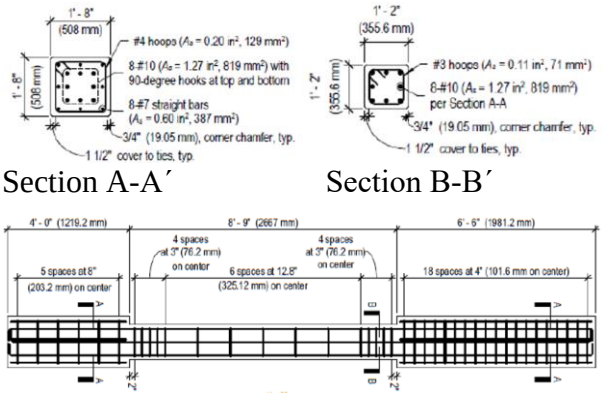

Figure 5: Test specimen geometry for UC Berkeley cyclic column.

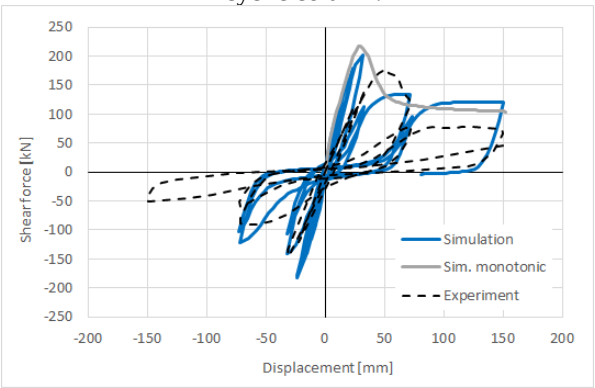

Figure 6: UC Berkeley cyclic test result comparison.

ATENA software was used in one of the winning predictions in the student category by Sasan Dolati, Ph.D. student from University of Texas at San Antonio. The load-displacement curves including the predictions by the authors are shown in Figure 6. The prediction was quite satisfactory even though the initial stiffness of the system is significantly overestimated, which can be attributed to higher flexibility of the boundary conditions in the experiment. Material variability was not addressed in the competition. The failure mode (see Figure 7) was also in a very good agreement with the experiment, where shear failure in diagonal tension in the middle section was reported.

Table 3: Material parameters for the UC Berkeley shear column.

Parameter	Value
Concrete	
Elastic modulus **E** [MPa]	26 012
Poisson ratio	0.2
Compressive strength $\mathbf{f_c}$ [MPa]	17.71
Tensile strength $\mathbf{f_t}$ [MPa]	1.37
Fracture energy $\mathbf{G_F}$ [N/m]	122
Crushing lim. displ. $\mathbf{w_d}$ [mm]	2.0
Fixed cracks	1.0
Strength reduction of cracked concrete r_c^{lim}	1.0
Crush band min [mm]	356
Shear factor S_F	20
Volume dilation β [-]	0.5
Reinforcement	
Elastic modulus **E** [MPa]	200 000
Yield strength $\mathbf{f_{ys}}$ [MPa]	478(*)/379(**)
Tensile strength $\mathbf{f_{ts}}$ [MPa]	680(*)/568(**)
Limit strain ε_{s2} [-]	0.188/0.21(**)
(*) Reinforcement #7 and #10	
(**) Hoop reinforcement #3 and #4	

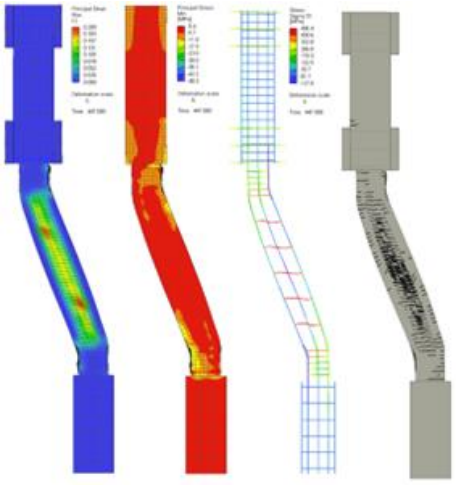

Figure 7: Failure modes in the UC Berkeley cyclic column numerical simulation.

3.3 Pre-stressed beam TU Delft

TU Delft organized a prediction contest in the spring of 2023 for full scale tests of precast continuous concrete inverted T beams. The specimens were designed to represent a typical multi-span girder in existing bridges in the Netherland. Many detailing of these structures do not fulfill the requirements of the modern design codes, and therefore were subjected to more detailed investigation.

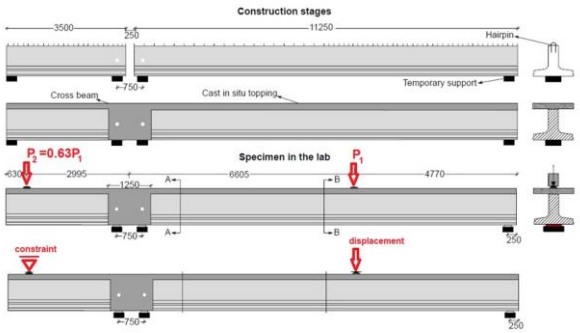

Figure 8: Geometry of the beam and their construction sequence tested at TU Delft beam prediction contest [24].

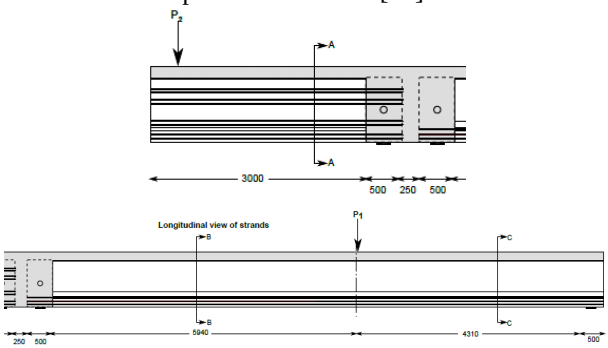

Figure 9: Geometry and pre-stressing tendons for the beam S10H1A.

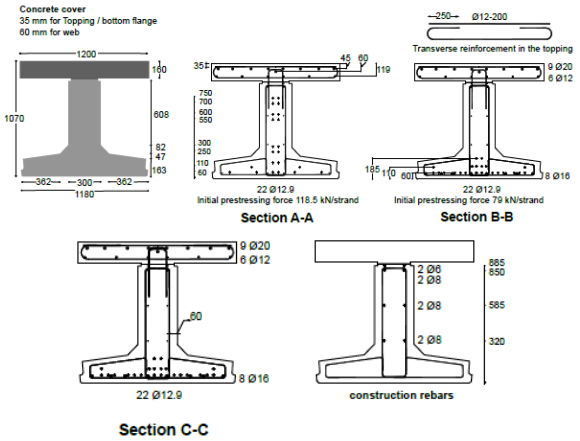

Figure 10: Cross-section and reinforcement arrangement for the beam S10H1A.

The details of the experiments are provided in [24]. The test consists of two precast beams that are later made continuous using cast-in-situ topping and cross beam. The construction stages and loading is described in Figure 8. The detailed geometry, reinforcement and tendon arrangement is shown in Figure 9 to Figure 12.

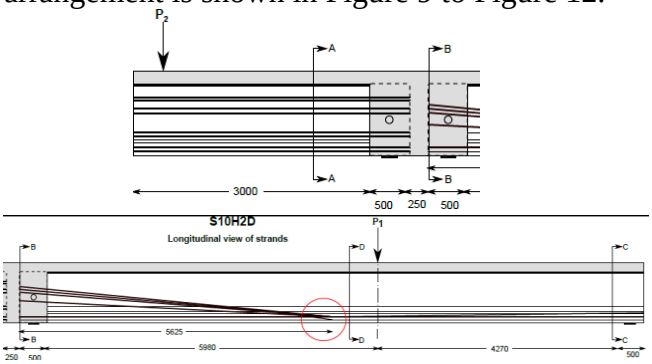

Figure 11: Geometry and pre-stressing tendons for the beam S10H2D for TU Delft contest.

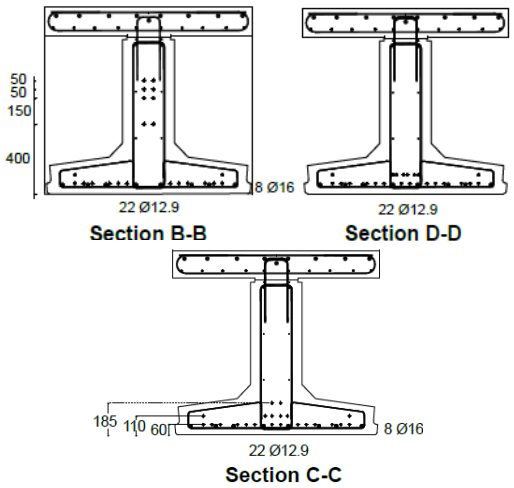

Figure 12: Cross-section and reinforcement arrangement for the beam S10H2D.

Two different continuous beams are tested. The specimen S10H1A has straight strands in the longer section with individual prestressing 79kN, while the specimen S10H2D has a fan-shape strands with the prestressing of 118.5 kN. The short cantilever beams of both cases are identical with the prestress 118.5 kN and shear reinforcement to prevent a shear failure. Another major difference between the two beams is the diameter of hairpin reinforcement in the interface along the top edge of the beam web (Ø6 – S10H1A, Ø12 – S10H2D).

Material properties for concrete, i.e. compressive strengths, were provided at 1st, 7th and 28th day. These values were used to interpolate up to the age of testing of 150 days

for S10H1A and 210 days for S10H2D using fib model code formulas. The resulting compressive strength values were used to estimate the other concrete parameters for the nonlinear analysis (see Table 4, Table 5,Table 6).

The comparison of the calculated load-displacement diagrams are shown in Figure 13 and Figure 14. The results show quite a good match for S10H2D with overprediction by about 8%. Very large overestimation of the peak load was obtained for the beam S10H1A. This can be largely attributed to a modelling error, by not specifically introducing an interface with reduced properties between the cast in situ top flange and the precast beam web. In the prediction analysis, it was assumed that a very good connection was achieved. The experimental results showed that the contact between the precast and cast in situ concrete was the critical location in both cases.

Table 4: Material parameters for concrete for the TU Delft contest.

Parameter	S10H1A	S10H1D	Cantilever
Concrete			
Elastic modulus **E** [MPa]	43 877	46 278	45 034
Poisson ratio		0.2	
Compressive strength $\mathbf{f_c}$ [MPa]	85	99.7	91.9
Tensile strength $\mathbf{f_{ct}}$ [MPa]	4.77	5.08	4.92
Fracture energy $\mathbf{G_F}$ [N/m]	162	167	165
Fixed cracks		0.7	
Strength reduction of cracked concrete r_c^{lim}		0.4	
Shear factor S_F		20	
Crushing lim. displ. $\mathbf{w_d}$ [mm]		2 / 0.2(*)	
Volume dilation b [-]		0.5	

This interface effect was not so pronounced in the S10H2D case due to the stronger hairpin reinforcement in this area. When interface elements were introduced in the critical zone with reduced tensile properties very good agreement was obtained (Figure 13).

Table 5: Material parameters for reinforcement for the TU Delft contest.

Rebar description	d [mm]	E_s [GPa]	f_y [MPa]	f_t [MPa]	ε_{s2} [-]
Shear reinf. web and hairpin	6	197	524	603	0.06
Shear reinf. bottom flange	8	199	539	618	0.06
Hairpin	12	204	524	605	0.05
Reinf. bottom flange	16	213	524	642	0.11
Reinf. top flange	20	198	593	702	0.08
	25	200	543	647	0.08
	12	203	536	605	0.06

Table 6: Material parameters for prestressing strands for the TU Delft contest.

Prestressing steel type	d [mm]	Nom. area [mm^2]	f_t [MPa]	ε_{s2} [-]	Relax. [-]
7-Wire strand	12.9	100	1860	0.035	0.045

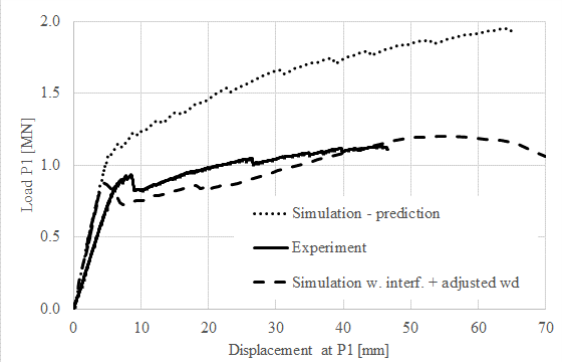

Figure 13: Comparison of results for beam S10H1A for TU Delft contest.

It was interesting to observe that even in the overestimated prediction analysis, a correct failure mode was predicted, i.e. splitting crack along the top web edge (Figure 15 and Figure 16), but reduction of the interface tensile properties was necessary to have a better match.

In the second case, the prediction analysis predicted a splitting crack below the hairpin reinforcement, which was slightly below the experimental crack pattern. It should be also

noted that the deflections are not predicted accurately, due to the fact that the experimental measurements include the deformation of the supports, which was not known and not taken into account in the analysis.

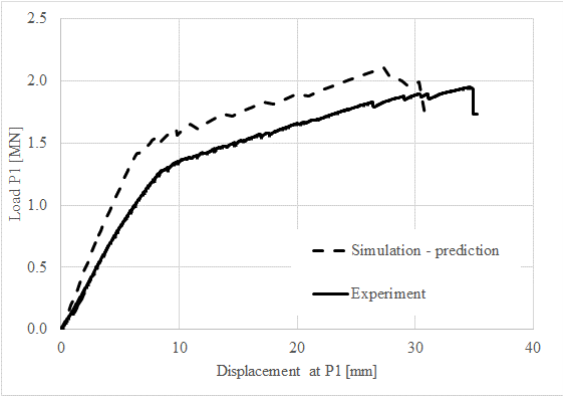

Figure 14: Comparison of results for beam S10H2D for TU Delft contest.

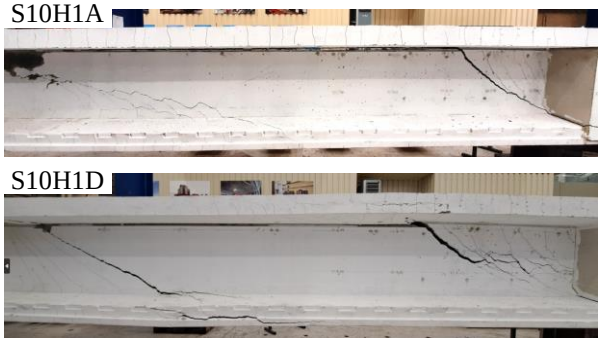

Figure 15: Deformed shape and failure modes from the experiment of TU Delf contest [24].

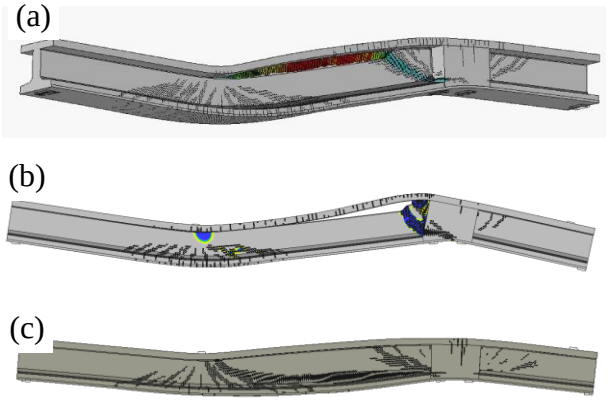

Figure 16: Deformed shape and failure modes from the simulation of TU Delf contest (a) S10H1A – prediction, (b) S10H1A – w. interf. and adjusted w_d, (c) S10H1D – prediction, blue areas indicate concrete crushing.

3.4 FRC shear beam *fib* WG 2.4.2

Several blind competitions have been organized recently by fib WG 2.4.2. Authors participated in one of the competitions involving a shear failure of a T-beam subjected to three-point bending and made of fibre-reinforced concrete. Details about the competitions and its results can be found in [25]. The geometry of the specimen and the reinforcement arrangement are shown in Figure 17.

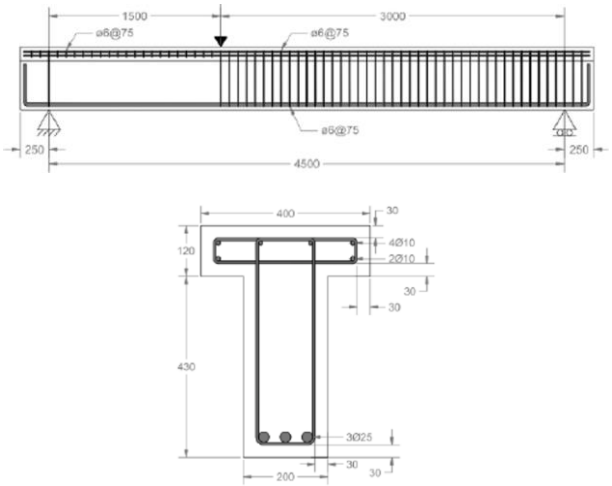

Figure 17: Geometry of the shear beam tested by Barros, fib WG 2.4.2

The material parameters used in the prediction analysis by ATENA are shown in Table 7. An important parameter for FRC analysis is the shape of the tensile softening diagram. Compared to other blind competitions, the organizers spent a significant effort to provide more information on material parameters. In addition to concrete compressive strength, experimental data were provided for standard notched three-point bending tests. Six test data sets for available for 6 specimens at 7 and 14 days. These tests could be used to calibrate the tensile stress strain relationship (see Figure 19 and Figure 20) to be used in the T-beam blind prediction. It should be noted that in ATENA application of the FRC tensile diagram (Figure 19), a scaling is applied to take into account the size of the finite element as shown in Figure 18, where ε_{loc} is an input parameter indicating the onset of localization, i.e. set to 0.0 for these analyses. L_t represents the crack band size, i.e. size of the finite element perpendicular to the crack direction, which is adjusted by mesh orientation factor [26][15]. L_{ch}^{t} is the size, for which the tensile diagram is valid. In this case, is equivalent to

the finite element size used in the three-point bend test calibration (Figure 20).

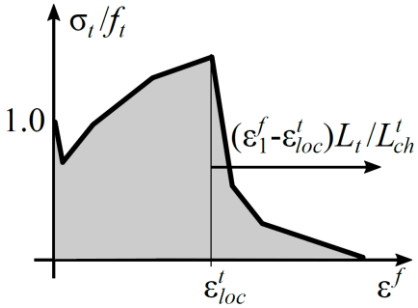

Figure 18: Scaling of the strain hardening/softening diagram for FRC concrete.

Table 7: Material parameters for the FRC shear beam contest, fib WG 2.4.2.

Parameter	Value		
Concrete			
Elastic modulus **E** [MPa]	33 000		
Poisson ratio	0.2		
Compressive strength $\mathbf{f_c}$ [MPa]	67		
Tensile strength $\mathbf{f_{ct}}$ [MPa]	5		
Fracture energy $\mathbf{G_F}$ [N/m]	see Figure 19		
Fixed cracks	1.0		
Strength reduction of cracked concrete r_c^{lim}	1.0		
Shear factor s_F	20		
Volume dilation b [-]	0.0		
Reinforcement	r25	r10	r6
Elastic modulus **E** [MPa]	200 000		
Yield strength $\mathbf{f_{ys}}$ [MPa]	550	538	527
Tensile strength $\mathbf{f_{ts}}$ [MPa]	678	696	700
Limit strain ε_{s2} [-]	0.075	0.075	0.075

In addition, two T-beams have been tested providing at least some information about the data scatter. The experimental and numerical load-displacement curves are shown in Figure 21. It is possible to observe that the prediction analysis ("Fit to mean – prediction") significantly overestimated the peak load and a wrong failure mode was obtained. Even though, strong diagonal shear cracking has developed in the model, due to the significant effect of fibers bridging the crack, the final failure mode was bending failure due to yielding of the bottom reinforcement (see Figure 22c).

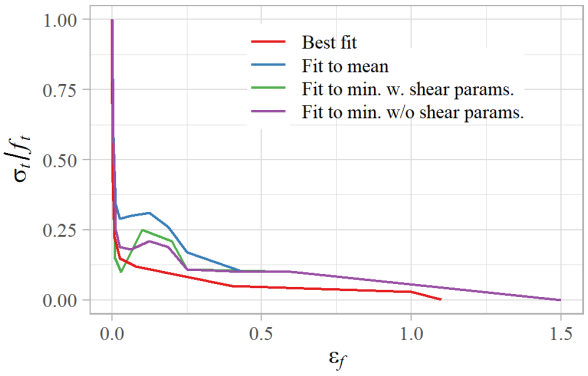

Figure 19: Comparison of the used stress-strain relationship for the FRC shear beam contest.

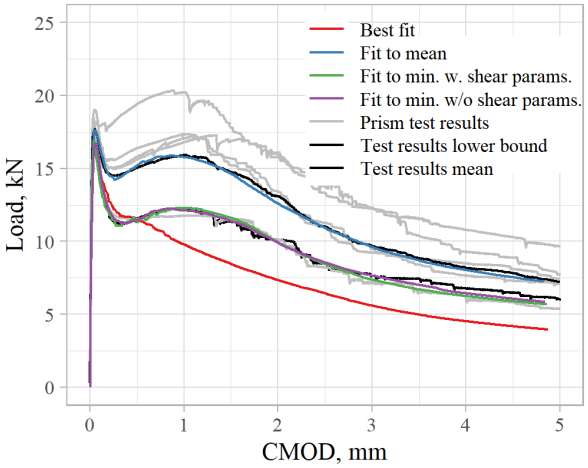

Figure 20: Comparison of load-displacement diagrams for the notched three point bend test for the model calibration for FRC shear beam contest.

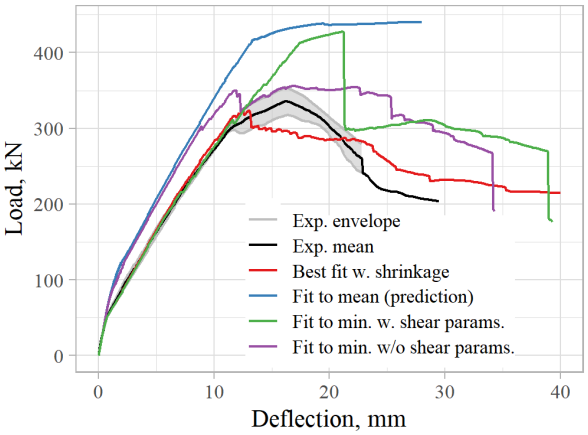

Figure 21: Comparison of main results for the FRC shear beam contest.

More detailed study [26] that has been performed after the publication of the competition results revealed two main sources of this overestimation:

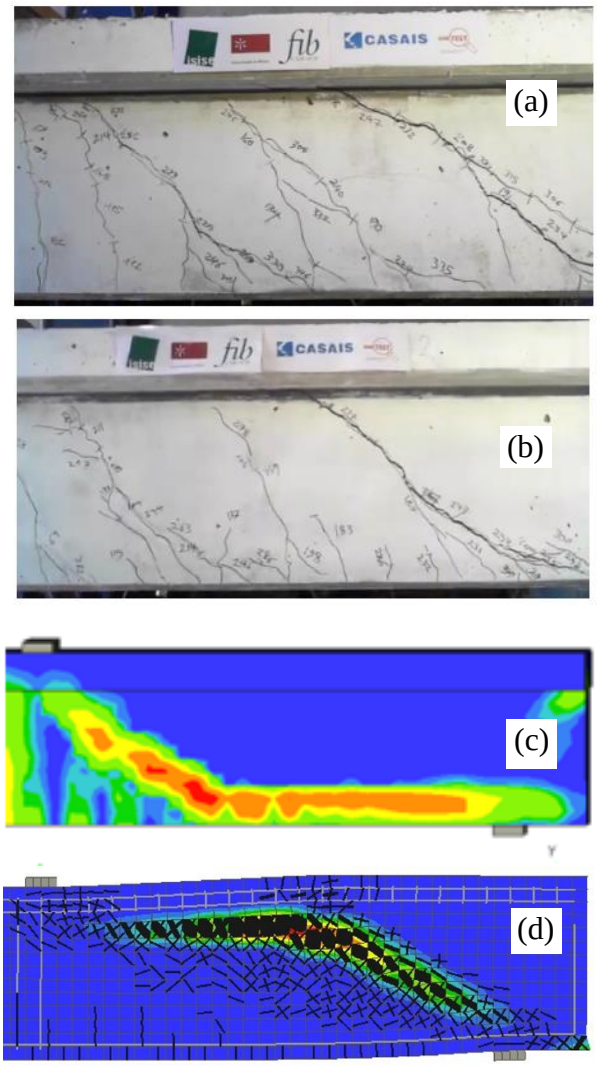

Figure 22: Comparison of crack patterns, (a-b) experiment, (c) initial prediction, (d) fit to minimum.

Fracture-plastic material model in software ATENA for FRC material requires the definition of shear retention factor and shear strength of the crack concrete. In the prediction analysis, these curves were left to their default values rather than being adjusted to reflect the actual shape of the tensile stress-strain diagram that was determined by fitting the notched three-point bend tests (see Figure 19 and Figure 20).

Another important factor was the consideration of the scatter of results in the notched three-point bend tests. Significant improvement in the results was obtained if the tensile diagram (Figure 19) was fitted to the lower bound of the three-point bend tests (Figure 20).

The post-competition study [26] also revealed that in order to capture correctly the pre-peak response it was also important to consider the shrinkage in the experiment corresponding to the relative humidity of 50%, i.e. shrinkage strain -0.18‰ and -0.24‰ for the web and flange respectively.

4 CONCLUSIONS

The accuracy of the investigated blind competition predictions are summarized in Table 8.

The table also highlights the most important deficiencies and drawbacks in the presented blind competitions. Material uncertainty is typically not considered, with the exception of the fib WG 2.4.2 competition, where at least two beams were tested, and statistical properties of the basic material tests were available. The second problem, which is typical for most blind competitions, is the availability of only basic material parameters for concrete. Typically, only concrete compressive strength is available, while for accurate modelling of concrete structures at least tensile strength and fracture energy would be necessary. The only exception is the FRC shear beam blind competition organized by fib WG 2.4.2, where notched three-point bend tests were available for the calibration of the material model parameters.

The Table 8 shows that in most cases the obtained error is acceptable or at least on the safe side. The only exception is the beam S10H1A from the TU Delft contest, which was overestimated by 69%. It can be argued that this error was mainly due to a modelling error of not assuming the reduced interface properties between the prefabricated inverted T-beam and the cast in-situ top flange.

In the case of the FRC shear beam, the overestimation was also partly caused by a modelling error, where the shear properties of the cracked concrete were not adjusted based on the calibrated tensile stress-strain diagram. It was also shown that more accurate results are obtained if the material parameters calibration

is performed using the lower bound data from the notched three-point bend tests.

This analysis of the blind prediction competitions have been performed as part of the research project TM04000013 "Virtual modelling of green concrete - structures with novel multi-spiral reinforcement and steel members" funded under the program DELTA 2 by the Czech Technology Agency.

Table 8: Summary of blind competition experience

Competition	Error [%]	Note
Large shear beam, Toronto 2015	+6 -8.5	Self weight should be considered, Material uncertainty not included, Limited concrete material parameters **(Excellent match)**
Large shear beam, Berkeley 2021	-25 -22	Self weight should be considered, Material uncertainty not included, Limited concrete material parameters **(Assumption of shrinkage reduced prediction)**
Shear column, Berkeley 2021	+16	Material uncertainty not included, Limited concrete material parameters **(Reasonable match)**
Prestressed prefabricated beam TU Delft 2023	+69 +8	Material uncertainty not included, Limited concrete material parameters **(Effect of interface not considered, good match only in second case)**
FRC shear beam, Barros, fib WG 2.4.2	30	Material uncertainty partially addressed, Additional material tests available for calibration, **(Better fit if calibrated to lower bound material tests)**

REFERENCES

[1] Ngo, D., Scordelis, A.C. 1967. Finite element analysis of rein-forced concrete beams, J. Amer. Concr. Inst. 64, pp. 152-163.

[2] Rashid, Y.R. 1968. Analysis of prestressed concrete pressure vessels. Nuclear Engineering and Design 7 (4), 334-344.

[3] Červenka, V., Gerstle, K., 1971. Inelastic analysis of reinforced concrete panels. Part I : Theory. Publication I.A.B.S.E. 31 (11), 32-45.

[4] Suidan, M., Schnobrich, W.C. 1973. Finite Element Analysis of Reinforced Concrete, ASCE, J. of Struct. Div., Vol. 99, No. ST10, pp. 2108-2121

[5] Lin, C.S., and Scordelis, A. 1975. Nonlinear Analysis of RC Shells of General Form, ASCE, J. of Struct. Eng., Vol. 101, No. 3, pp. 152-163.

[6] de Borst, R. 1986. Non-linear analysis of frictional materials. PhD Thesis, Delft University of Technology, The Nether-lands.

[7] Rots, J.G., Blaauwendraad, J. 1989. Crack models for concrete : Discrete or smeared, Fixed, multi-directional or rotating? Heron 34 (1).

[8] Pramono, E., Willam, K.J. 1989. Fracture energy-based plastici-ty formulation of plain concrete. J. of Eng. Mech., ASCE 115 (6), 1183-1204.

[9] Etse, G. 1992. Theoretische und numerische untersuchung zum diffusen und lokalisierten versagen in beton. PhD Thesis, University of Karlsruhe.

[10] Lee, J., Fenves, G.L. 1998. Plastic-damage model for cyclic loading of concrete structures. J. of Eng. Mech., ASCE 124 (8), 892 – 900.

[11] Červenka, J., Červenka, V., Eligehausen, R. 1998. Fracture-Plastic Material Model for Concrete, Application to Analysis of Powder Actuated Anchors, FRAMCOS 3, 1998, pp 1107-1116.

[12] Bažant, Z.P. & Oh, B.H., 1983. Crack band theory for fracture of concrete. Materials and Struct., RILEM 16 (3), 155–177.

[13] Model Code 2010. 2011. fib Lausanne, Ernst & Sohn: Switzerland
[14] Červenka V, Červenka J, Kadlec L. 2018. Model uncertainties in numerical simulations of reinforced concrete structures. Struct. Concrete; 19(6): 2004 https://doi.org/10. 1002/suco.201700287.
[15] Červenka, V., Červenka, J. & Jendele, L. 2021. ATENA Pro-gram Documentation, Part 1: Theory, 2021, Cervenka Consulting s.r.o., www.cervenka.cz
[16] Červenka J. & Papanikolaou V. 2008. Three Dimensional Combined Fracture-Plastic Material Model for Concrete. Int J. of Plast. 24:2192-220.
[17] Engen M, Hendriks M., Köhler J, Øverli JA, Åldtstedt E. 2017. A quantification of modelling uncertainty for non-linear finite element analysis of large concrete structures. Struct. Safety 2017; 64: 1-8.
[18] Castaldo, P., Gino, D., Bertagnoli, G., Mancini, G. 2018. Partial safety factor for resistance model uncertainties in 2D non-linear analysis of reinforced concrete structures, Eng. Struct., 176, 746-762. https://doi.org/10.1016/j.engstruct.2018.09.041.
[19] Castaldo, P., Gino, D., Bertagnoli, G., Mancini, G. 2020. Re-sistance model uncertainty in non-linear finite element analyses of cyclically loaded reinforced concrete systems, Eng. Struct., 211(2020), 110496, https://doi.org/10.1016/j.engstruct.2020.110496
[20] Gino D, Castaldo P, Giordano L, Mancini G. 2021. Model un-certainty in nonlinear numerical analyses of slender rein-forced concrete members. Struct. Concrete. 1–26. https://doi.org/10.1002/suco.202000600
[21] Collins, M.P., Bentz, E.C., Quach, P.T. & Proestos, G.T., 2015, Challenge of Predicting the Shear Strength of Very Thick Slabs. Concrete Int., V.37,No.11, Nov. 2015, pp 29-37.
[22] Moehle J., Zhai, J. 2021. Thick foundation element blind pre-diction contest, https://peer.berkeley.edu/news-and-events/2021-thick-foundation-element-blind-prediction-contest
[23] Gunay, S., Donald, E., 2021. Reinforced Concrete Column Blind Prediction Contest, https://peer.berkeley.edu/news-and-events/2021-reinforced-concrete-column-blind-prediction-contest
[24] Ibrahim, M.S., Kostense, N.W., Poliotti, M., Yang, Y., 2023, TU-Delft blind prediction contest on prestressed concrete beams made continuous, https://concrete-prediction-contest.tudelft.nl
[25] Barros, et al. 2020, Blind competition on the numerical simulation of steel-fiber-reinforced concrete beams failing in shear, Struct. Concrete, Journal of the fib, 2020, https://doi.org/10.1002/suco.202000345
[26] Červenka, V., Margoldová, J., 1995, Tension Stiffening Effect in Smeared Crack Model, Eng. Mech., S. F. Sture (Eds), Proc. 10th Conf., Boulder, Colorado, pp. 655-658.
[27] Skadins U., Cervenka, J., Lessons learnt from blind competition of shear behavior of fiber reinforced concrete T-beam, Struct. Concrete, Journal of the fib, 2023, https://doi.org/10.1002/suco.202201187
[28] Houlin, X., Donmez A.A., Nguyen, H.T. Bazant, Z.P., What We Can and Cannot Learn from a Single Shear Test of a Very Large RC Beam, J. of Struct. Eng., 149 (9), 2023, https://doi.org/10.1061/JSENDH.STENG-12242